Magnetoresistance scaling in MBE-grown $La_{0.7}Ca_{0.3}MnO_3$ thin films

J. O'Donnell, M. Onellion, and M. S. Rzchowski
Department of Physics, University of Wisconsin-Madison, 1150 University Avenue, Madison, Wisconsin 53706

J. N. Eckstein and I. Bozovic
Varian Research Center, 3075 Hansen Way, Palo Alto, California 94304
(Received 19 June 1996; revised manuscript received 17 July 1996)

We present a detailed analysis of magnetoresistance in tetragonal thin films of ferromagnetic $La_{0.7}Ca_{0.3}MnO_\delta$ grown by atomic layer-by-layer molecular-beam epitaxy. The field and temperature dependence of the resistivity ρ show an explicit dependence only on the fractional magnetization M/M_{sat} and are consistent with a single approximate form $\rho \approx \rho(0)\exp[-C(M/M_{sat})^2]$ for small and intermediate magnetization both above and below the Curie temperature (T_C). The microscopic magnetization and susceptibility (χ) have been inferred from the low-field magnetoresistance above T_C with χ following a Curie-Weiss form. We observe a sharp transition in the low-field (H) dependence of ρ from quadratic ($\propto H^2$) above T_C to linear ($\propto H$) below, consistent with a temperature-independent $\rho(M)$. Finally we show that within a simple model this temperature-independent form for ρ reproduces the behavior of the measured low-field sensitivity below T_C. [S0163-1829(96)52534-8]

Thin films of manganese perovskites have recently been shown to exhibit very large (''colossal'') magnetoresistance (CMR).[1,2] Theoretical efforts[3–5] have attributed this behavior, as well as the observed ferromagnetic transition, to strong-correlation effects between the Mn itinerant d-band e_g holes produced by A-site doping in ABO_3 and the localized e_g and t_{2g} d-band electrons as well as possible lattice interactions. Polaronic hopping has been suggested[3,5–7] as an explanation for the activated behavior of zero-field resistivity above the Curie temperature, with a delocalizing crossover to metallic behavior below. For small sample magnetization (predominantly above the Curie temperature), theories based on these considerations have predicted[4,8] a quadratic dependence of the magnetoresistance on magnetization with a curvature that depends on the hole doping, the e_g bandwidth, and the on-site Hund's coupling.[4] Experimental dependences of the magnetoresistance on the magnetization varying from exponential to power law have been reported in thin films,[7,9,10] although the entire temperature range about the Curie temperature (T_C) has not always been studied.

In this paper we report on extensive magnetoresistive characterization over a wide range of both temperature and applied magnetic field of $La_{0.7}Ca_{0.3}MnO_3$ films grown by atomic-layer-by-layer molecular beam epitaxy.[11,12] Our major result is a consistent interpretation of our temperature and field-dependent magnetoresistance data both above and below the ferromagnetic transition in terms of a resistivity dependent only on the magnetization. This dependence, which we find to be approximated by a Gaussian, does not substantially change with temperature despite the dramatic change in the temperature dependence of the resistivity from activated to metallic. We base this interpretation on a magnetoresistance above T_C that scales with temperature consistent with a Curie-Weiss susceptibility and gives an experimental indication of the dependence of resistivity on magnetization, a sharp transition in the low-field magnetoresistance from quadratic dependence on applied field above T_C to linear below, and an asymmetric peak in the temperature-dependence of the linear low-field sensitivity below T_C. Within this interpretation we also determine the factors that control the low-field sensitivity below T_C.

The films were grown on nearly {001} oriented atomically flat $SrTiO_3$ substrates. Accurate codeposition of the lanthanum, alkaline earth and manganese atoms was employed to ensure that the instantaneous surface population of mobile species would match the average film composition and minimize small scale composition variations. The films were grown at temperatures ranging from 650 to 750 °C, oxidized with a beam of pure ozone, and required to post-anneal. The samples were 58 nm thick. Atomic force microscopy shows atomically flat surfaces that are interrupted by occasional 4 Å steps, i.e., atomically terraced surfaces that are replicas of the substrate. There are no AFM indications of grain boundaries in the material, similar to other recently reported MBE films.[13] X-ray diffraction data indicate that these films possess a tetragonal unit cell with in-plane lattice constant of 0.390 nm (consistent with that of the $SrTiO_3$ substrate), and a perpendicular lattice constant of 0.383 nm. The pseudomorphic match to the $SrTiO_3$ indicates that the film is strained throughout its thickness, resulting in the tetragonal structure.

The samples were patterned into 100 μm wide wires for four-point measurements of five squares of the material. Figure 1 shows a typical zero-field resistivity and high-field magnetoresistance ratio $[\rho(0)-\rho(T)]/\rho(7T)$ as a function of temperature. The zero-field resistance shows the high-temperature activated and low-temperature metallic behaviors in agreement with other reports.[1,2] The magnetoresistance ratio is sharply peaked with a width of approximately 25 K at a temperature slightly less than that of the zero-field resistivity peak. This report focuses on two samples, with resistivity peak temperatures (T_P) of 168 K and 151 K.

Magnetotransport measurements were made over a wide temperature range above and below T_P with the field applied

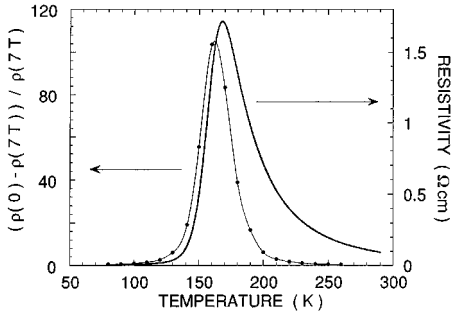

FIG. 1. Zero field resistivity and high-field magnetoresistance for a pseudomorphic tetragonal thin film of $La_{0.7}Ca_{0.3}MnO_3$. The solid line through the high-field sensitivity points is a guide to the eye.

in the plane of the film and parallel to a transport current oriented along the $\{100\}$ direction of the film. Figure 2 shows the field-dependence of the normalized magnetoresistance of the $T_P=168$ K sample for 10 K increments of temperature roughly below (2a) and above (2b) T_P. Magnetization measurements of similarly prepared samples with $T_p\sim 145$ K indicate that T_C is a few K above T_P. Most immediately noticeable is a change in the low-field response from predominantly quadratic $(\partial\rho/\partial H|_{H=0}=0)$ for $T>T_P$ to linear $(\partial\rho/\partial H|_{H=0}<0)$ for $T<T_P$ as noted previously in thin films.[14,15] In the following, we test a simple model displaying the general magnetotransport symmetries[15] that can lead to this behavior by fitting the experimental data and physically interpreting the resulting parameters.

Above T_P (and hence above T_C) the magnetization is small in laboratory-scale fields and lowest-order models predict[4,5,8]

$$\rho(M)=\rho(M=0)[1-C(M/M_{\rm sat})^2]. \tag{1}$$

Here $M_{\rm sat}$ is the spin-aligned magnetization, M the local magnetization, ρ the resistivity, and C a parameter with no explicit temperature or field-dependence. C is however predicted to depend on the Hund coupling, the hole bandwidth, and the hole concentration.[4] This behavior would appear as a positive quadratic term in the conductivity.[14,16] We stress here that due to the short mean-free path in these materials M should be interpreted as the magnetization within a single domain, and not the domain-averaged sample magnetization. This M is accessible through magnetization measurements only for applied fields sufficiently above the coercive field

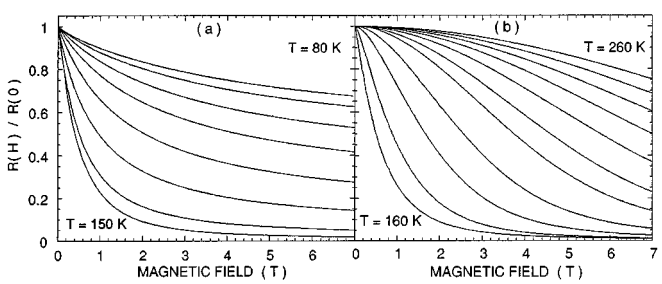

FIG. 2. Field dependence of the magnetoresistance for temperatures below (a) and above (b) the resistivity peak, illustrating the crossover from linear to quadratic low-field behavior.

that the sample is a single magnetic domain. Writing the magnetization as $M(H)=M_0+\chi(T)H$ where M_0 is the spontaneous magnetization, χ the susceptibility, and H the applied field, the normalized resistivity from Eq. (1) becomes

$$\rho(H)/\rho(M=0)=1-(C/M_{\rm sat}^2)(M_0^2+2\chi M_0 H+\chi^2H^2). \tag{2}$$

This model reproduces the experimentally-observed crossover from low-field magnetoresistance quadratic in H above T_C to linear below T_C as simply a growth of a finite spontaneous magnetization without a change in the physical mechanism of magnetoresistance described by Eq. (1). The model however also predicts a negative curvature of $\rho(H)$ at all temperatures. The data of Fig. 2 show positive curvature below T_C, indicating that the small M limit of Eq. (1) is rapidly exceeded. This temperature range below T_p is discussed later in more detail, and is shown to be consistent with a more complex but still temperature-independent $\rho(M)$.

Above T_p we quantitatively test the theoretically predicted result of Eq. (1) by fitting our low-field magnetoresistance data to

$$\rho(H)=\rho(M_0,H=0)(1-a|H|-bH^2) \tag{3}$$

and extracting the temperature-dependent fit parameters a and b. Using Eq. (2), the susceptibility χ and spontaneous magnetization M_0 can then be determined from the magnetoresistance data:

$$C^{1/2}(\chi/M_{\rm sat})=2b/\gamma, \quad C^{1/2}(M_0/M_{\rm sat})=a/\gamma, \tag{4}$$

where $\gamma=(a^2+4b)^{1/2}$. The resultant normalized inverse susceptibility is shown in Figs. 3(a) and 3(b) for the $T_P=168$ K and $T_P=151$ K samples respectively. The linear fits illustrate Curie-Weiss behavior with paramagnetic Curie temperatures (T_c^p) of 176 K ($T_P=168$ K) and 166 K ($T_P=151$ K), indicating that the parameter C has at most a weak temperature dependence. The insets show semilog plots of the small apparent spontaneous short-range magnetization M_0 above T_P. The multiple data points at some temperatures indicate the spread in fit parameters resulting from different field ranges for the fit.

We further probe these effects using the Curie-Weiss form for the susceptibility obtained from the data and its expected magnitude. The scaled inverse susceptibility of Eq. (4) can then be written using the standard Curie-Weiss form with an approximate average moment[16] resulting in

$$(C^{1/2}\chi/M_{\rm sat})^{-1}=[3k_B/C^{1/2}g\mu_B(S_{\rm ave}+1)](T-T_C^p) \tag{5}$$

where k_B is Boltzmann's constant, $S_{\rm ave}$ is the average spin, $g=2$, μ_B is the Bohr magneton, and a saturation magnetization of $(N/V)\mu_B S_{\rm ave}$ has been used. With $S_{\rm ave}=1.85$ $(x=0.3)$ we find that $C^{1/2}\approx 5$, a value substantially larger than the values of 1.4–2 reported for bulk single crystal LSMO[17] and bulk ceramic Y-substituted LCMO.[18] This value for $C^{1/2}$ and the insets to Figs. 3(a) and 3(b) indicate that 10 K above T_p $M_0/M_{\rm sat}\approx 0.004$ $(T_p=168$ K) and $M_0/M_{\rm sat}\approx 0.015$ $(T_p=151$ K). This is consistent with our observations of low-field (100 Oe) hysteresis[19] persisting to ~ 15 K above T_p for these samples, and requires a magnetization that is static on the several minute time scale of the hysteresis measurement. The insets show that the M_0 are

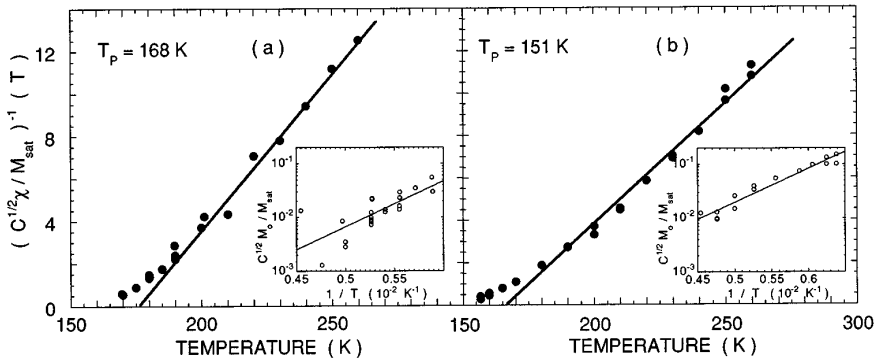

FIG. 3. Extracted inverse normalized susceptibility (main figures) and spontaneous magnetization (insets) for samples with (a) $T_P = 168$ K and (b) $T_P = 151$ K. The linear fit indicates Curie-Weiss behavior.

consistent with an activated form with activation energies of 165 ± 35 meV ($T_p = 168$ K) and 125 ± 10 meV ($T_p = 151$ K). These energies are similar to our measured high-temperature activation energies of the zero-field resistivity (~ 120 meV). Similar activated magnetization above T_P has recently been observed in EPR powder measurements.[20] Due to the previously mentioned short mean-free path, we expect that the magnetoresistance probes the magnetization on a very short length scale. Our data indicate that the measured M_0 represents static short range magnetic order in the sample above T_p. Our measurement of T_P variations of less than 0.5 K between two wires separated on the same substrate by 500 μm suggests good sample uniformity, although we cannot rule out very short-range compositional fluctuations.

The value of C in Eq. (1) is expected to depend on the doping state and band structure of the sample. Equation (5) shows that a comparison of slopes between Figs. 3(a) and 3(b) is a direct comparison of the parameter C apart from the weak doping dependence of S_{ave}. The data show that the sample with higher T_p exhibits a smaller $C^{1/2}(S_{\text{ave}}+1)$ (larger slope). Within the theoretical interpretations of Refs. [3–5] a decrease in $C^{1/2}(S_{\text{ave}}+1)$ is due predominantly to an increasing hole concentration, consistent with a higher T_p.

These results show that the low-field behavior of the magnetoresistance above T_p is well represented by Eq. (1) and a linear dependence of magnetization on field. For magnetization outside the valid range of Eq. (1) we extract $\rho(M)$ directly from the data. Figure 4 shows the data of Fig. 2(b) vs $\chi H/M_{\text{sat}}$ with χ/M_{sat} determined from Fig. 3. Within the linear response regime, the horizontal axis is M/M_{sat}. Using this scaling the high-temperature data ($\geqslant 200$ K) collapse onto a single temperature-independent curve. The most straightforward interpretation of this collapse indicates that the magnetization is in the linear-response regime for $M \lesssim 0.2 M_{\text{sat}}$ and $T > 1.2 T_C$, and that $\rho(M)$ is largely temperature-independent. This single curve, similar to that reported for bulk LSMO[17] with a much higher T_p, then represents a temperature-independent $\rho(M)$ that consistently extends the small-magnetization approximation [Eq. (1), dashed line in Fig. 4] to larger magnetizations. The 190 K data of Fig. 4 shows a deviation of the scaled data indicating a high-field susceptibility smaller than the low-field estimate of Fig. 3: the magnetization has begun to saturate at these applied fields as T approaches T_c. Figure 4 remains consistent with a temperature-independent $\rho(M)$.

Below T_c the spontaneous magnetization rapidly becomes large enough that Eqs. (1) and (2) no longer hold. However, we can use the experimental $\rho(M)$ to interpret this temperature range by expanding the field-dependent resistivity about the spontaneous magnetization (valid for small H):

$$\rho(H) = \rho(M_0) + \left.\frac{\partial \rho}{\partial M}\right|_{M_0} \chi H + \left.\frac{1}{2}\frac{\partial^2 \rho}{\partial M^2}\right|_{M_0} (\chi H)^2 + \cdots . \qquad (6)$$

The experimental data of Fig. 4 shows that $\partial\rho/\partial M = 0$ at $M = 0$, leading to a decrease in ρ initially quadratic with H for $T > T_C$. An increase in spontaneous magnetization M_0 below T_c produces a nonzero $\partial\rho/\partial M|_{M_0}$ (Fig. 4). Combining this result and Eq. (6) leads to a predominantly linear behavior of $\rho(H)$, consistent with the data of Fig. 2. This mechanism is similar to that predicted by Eq. (2), but is not restricted to small magnetization. The change in local curvature of $\rho(M)$ from negative to positive at $M_0 \gtrsim 0.1 M_{\text{sat}}$ in Fig. 4 leads to a positive curvature in $\rho(H)$ as the applied field is increased below T_C where the magnetization is large. This is consistent with the previously noted appearance of positive curvature beyond the linear re-

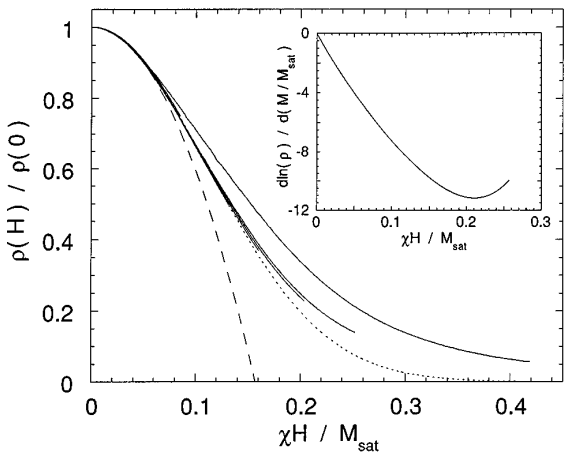

FIG. 4. Magnetoresistance shown in Fig. 2(b) vs field scaled by the susceptibility of Fig. 3(a) for temperatures of 190 through 260 K in 10 K increments. Dashed line indicates predicted low-field quadratic dependence. Dotted curve indicates phenomenological Gaussian $\exp(-CM^2)$ form. Scaling behavior of the seven highest-temperature curves indicate a temperature-independent form for the magnetoresistance above T_C. Inset shows logarithmic derivative of the 200 K data (see text).

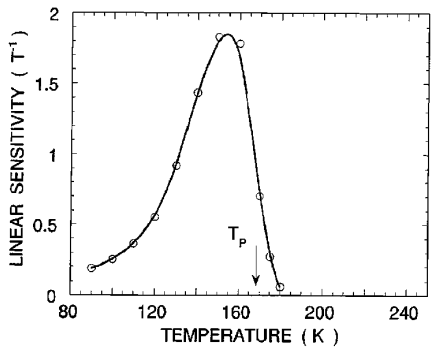

FIG. 5. Normalized linear magnetoresistance sensitivity $|(1/\rho)(\partial\rho/\partial H)|_{H=0}|$ as a function of temperature for the sample of Fig. 1. The solid curve is a guide to the eye.

gime in the experimental magnetoresistance (MR) below T_p (Fig. 2). This analysis shows that the general features of the magnetoresistance are consistent with a temperature-independent $\rho(M)$. We now use this approach to analyze the temperature range below T_C in more detail.

The linear dependence of $\rho(H)$ dominates the low-field sensitivity below T_p. The temperature-dependence of the normalized linear slope ($|(1/\rho)\partial\rho/\partial H|$) of the data in Figs. 2(a) and 2(b) at $H=200$ Oe is shown in Fig. 5. It peaks at approximately the same temperature as the high-field MR ratio (Fig. 1) but is asymmetric and at low temperatures decreases much more slowly than the high-field MR ratio. Here we concentrate on the low-field sensitivity where a linear-response approach is valid.

Equation (6) predicts that the linear low-field response can be written $\chi(M_0)\partial\ln\rho/\partial M|_{M_0}$ showing that its temperature dependence is controlled by three factors: $M_0(T)$, $\chi(M_0)$, and $\partial\ln\rho/\partial M|_{M_0}$. The inset of Fig. 4, calculated from the 200-K data of Fig. 4, shows that the absolute value of the last factor initially increases approximately linearly with M_0. $\chi(M_0)$ generally decreases with increasing M_0 and can be shown within mean field to give $\chi=-(t/\lambda)\partial\ln(M_0/M_{\rm sat})/\partial t$, where $t=T/T_C$ is the reduced temperature and λ is the mean-field coupling. At small and intermediate magnetization, the data is fit reasonably well by $\rho(M_0)\approx\rho(M=0)\exp[-C(M_0/M_{\rm sat})^2]$ (shown as the dotted line in Fig. 4). This approximate form gives a normalized linear sensitivity proportional to $t\partial M_0/\partial t$ and is consistent with the data of Fig. 5 in two respects: (a) a strong peak near T_C and (b) a relatively slow decrease at low temperature [the approximate form gives a sensitivity $\propto t^\alpha$ for a low-temperature magnetization $M_0\approx M_{\rm sat}(1-\gamma t^\alpha)$ (Ref. 21)]. The inset to Fig. 4 indicates a ρ deviating from Gaussian behavior at $\chi H/M_{\rm sat}\approx 0.15$. Although we cannot rule out a slightly nonlinear $M(H)$ as the cause, the scaling observed in Fig. 4 suggests that the deviation is intrinsic. Our results and analysis show that the temperature dependence of the low-field linear sensitivity can be controlled below T_C through $M(T)$. We have in fact grown samples in which the linear sensitivity shows only 10% variations over a 60 K temperature range below T_C.

In summary, our data and analysis indicate that the temperature and magnetic field dependence of the magnetoresistance are consistent with a temperature-independent $\rho(M)$, which we have extracted from the experimental data. Because of nonuniversal temperature dependencies of the magnetization and susceptibility, it is not possible for us to rule out subtle changes in $\rho(M)$ below T_C. However, drastic temperature-dependent changes in $\rho(M)$ are not required to explain the experimental data above and below T_p and in fact are inconsistent with the data. In addition, we have presented what is to our knowledge the first use of magnetoresistance data to establish a Curie-Weiss form for χ above T_C. We have also used this magnetoresistance data to infer a short-range magnetization above T_C. Finally, within a simple model we have identified the factors that control the low-field sensitivity.

This work is supported by the Office of Naval Research through Contract Nos. N00014-940-C-0011 and N00014-94-1-0237.

[1] R. von Helmolt *et al.*, Phys. Rev. Lett. **71**, 2331 (1993).
[2] M. McCormack *et al.*, Appl. Phys. Lett. **64**, 3045 (1994); S. Jin *et al.*, Science **264**, 413 (1994).
[3] H. Roder, J. Zang, and A. R. Bishop, Phys. Rev. Lett. **76**, 1356 (1996); Jun Zang, A. R. Bishop, and H. Roder (unpublished).
[4] N. Furukawa J. Phys. Soc. Jpn. **63**, 3214 (1994); **64**, 3164 (1995); **64**, 2734 (1995).
[5] A. J. Millis, P. Littlewood, and B. I. Shraiman, Phys. Rev. Lett. **74**, 5144 (1995); A. J. Millis, R. Mueller, and B. I. Shraiman (unpublished).
[6] Y. X. Jia *et al.*, Phys. Rev. B **52**, 9147 (1995).
[7] M. Jaime *et al.*, Appl. Phys. Lett. **68**, 1576 (1996); J. Fontcuberta, *et al., ibid.* **68**, 2288 (1996).
[8] J. Inoue and S. Maekawa, Phys. Rev. Lett. **74**, 3407 (1995).
[9] M. F. Hundley *et al.*, Appl. Phys. Lett. **67**, 860 (1995).
[10] G. J. Snyder *et al.*, Phys. Rev. B **53**, 14 434 (1996).
[11] J. N. Eckstein and I. Bozovic, Annu. Rev. Mater. Sci. **25**, 679 (1995).
[12] J. N. Eckstein *et al.*, Appl. Phys. Lett. (to be published).
[13] V. A. Vas'ko *et al.*, Appl. Phys. Lett. **68**, 2571 (1996); V. S. Achutharaman *et al., ibid.* **67**, 1019 (1995).
[14] J. Z. Sun *et al.*, Appl. Phys. Lett. **67**, 2726 (1995).
[15] G. J. Snyder, R. Hiskes, S. DiCarolis, M. R. Beasley, and T. H. Geballe (unpublished).
[16] J. Nunez-Regueriro and A. M. Kadin, Appl. Phys. Lett. **68**, 2747 (1996).
[17] Y. Tokura *et al.*, J. Phys. Soc. Jpn. **63**, 3931 (1994).
[18] J. Fontcuberta *et al.*, Phys. Rev. Lett. **76**, 1122 (1996).
[19] J. O'Donnell, M. Onellion, M. S. Rzchowski, J. N. Eckstein, and I. Bozovic (unpublished).
[20] S. B. Oseroff *et al.*, Phys. Rev. B **53**, 6521 (1996).
[21] Such low-temperature power-law magnetization, observed experimentally in Ref. 10, can be a result of collective excitations.